

S024

Model-based PP-PS Joint Inversion - A Sensitivity Study on Method, Input Data Type, Initial Model and Noise Level

W. Yang (Geotrace Technologies) & J.H.Y. Yu* (Geotrace Technologies)

SUMMARY

we investigate two model-based prestack inversion methods: Simulated Annealing (SA) and Nonlinear Conjugate Gradient (CG) to simultaneously invert PP and PS prestack seismic data to three petroelastic parameters: V_p , V_s , and density. To properly test the methods and evaluate the results, various responses of a six-layer synthetic model with different parameters are computed and used as the input for inversion. The test procedure is designed to evaluate the impact of three key factors in a normal inversion workflow for these two inversion methods: (1) input data type, i.e., PP only, PS only or PP-PS jointly, (2) signal-to-noise ratio, and (3) initial model. In addition, we review the computation performance between two methods. From this controlled test environment we observe that (a) PP-PS joint inversion is more robust than the inversion of PP only or PS only, (b) both SA and CG are not greatly influenced by random noises, (c) SA method is less sensitive to the initial model than CG, (d) the inversion results of CG and SA are comparable but SA has an edge due to its global optimization, and (e) CG is much faster than SA in terms of computation not the result.

Introduction

It has been demonstrated that PP-PS joint inversion can produce more reliable result than PP or PS only inversion when exposed to noises (Veire and Landrø, 2006; Rabben et al., 2008). However, most of published joint inversion methods usually invert sample by sample for the reflection coefficients of petroelastic parameters. This approach has two shortcomings. One is that it produces the reflection coefficients, not the absolute values that geoscientists really need for detailed reservoir characterization and simulation. To obtain absolute values, one needs to integrate the coefficients for the high-frequency component and add the low-frequency component from logs or seismic velocities. This procedure can be tedious and prone to errors. The other weakness is that it treats the recorded PP and PS seismic amplitude data as the reflection coefficients. In fact, it requires well logs to calibrate the seismic amplitudes and make them closer to the geological reflectivity trend. Furthermore, it doesn't consider the constructive and destructive interference effect caused by the limited bandwidth nature of the wavelet in the seismic data. At the end, seismic amplitudes cannot truly represent the real geological reflection coefficients. For inversion, it can lead to errors.

In stead of sample by sample inversion, we propose a model-based inversion to simultaneously invert for the absolute values of P-wave velocity V_p , S-wave velocity V_s , and bulk density ρ using concurrently the seismic amplitude characteristics (i.e., amplitude versus offset or AVO) of all samples within a prestack migrated CMP gather. The inversion requires an initial model of V_p , V_s and ρ and a known wavelet. Then it perturbs the model and its model responses to match the seismic data with two optimization approaches: (1) global inversion using Simulated Annealing (SA) method and (2) local inversion using Nonlinear Conjugate Gradient (CG) method. We test and compare the impact of input data type, signal-to-noise ratio, and initial model as well as the result quality and the computation performance.

Theory

Aki and Richards' (1980) approximations of the Zoeppritz equations for PP reflection coefficients and PS reflection coefficients are given by

$$R_{PP}(\theta) \approx \left(1 - 4 \frac{V_s^2}{V_p^2} \sin^2 \theta\right) \frac{\Delta \rho}{2\rho} + \sec^2 \theta \frac{\Delta V_p}{2V_p} - 8 \frac{V_s^2}{V_p^2} \sin^2 \theta \frac{\Delta V_s}{2V_s}, \quad (1)$$

and

$$R_{PS}(\theta) \approx \frac{\sin \theta}{\cos \varphi} \left[4(\sin^2 \varphi - \gamma \cos \theta \cos \varphi) \frac{\Delta V_s}{2V_s} - (\cos 2\varphi + 2\gamma \cos \theta \cos \varphi) \frac{\Delta \rho}{2\rho} \right] \quad (2)$$

Where $\Delta V_p = (V_{p2} - V_{p1})$, $V_p = \frac{(V_{p1} + V_{p2})}{2}$ (similar for V_s and ρ), $\gamma = V_s/V_p$ (unlike others assume γ is known, we determine it through solving V_p and V_s), θ is the P-wave incidence angle, and φ is the S-wave incidence angle. These two angles are related by the Snell's law $\varphi = \sin^{-1}(\gamma \sin \theta)$.

Seismic traces as a function of two-way travel time and incident angle can be modeled by the convolution theory:

$$T_{PP}(\theta, t) = \int_{-\infty}^{+\infty} R_{PP}(\theta, \tau) W(t - \tau) d\tau, \quad (3)$$

where $T_{PP}(\theta, t)$ is a PP-wave seismic trace (similar for PS-wave $T_{PS}(\theta, t)$), $W(t)$ is the seismic wavelet, and $R_{PP}(\theta, t)$ is the reflection coefficients. This mathematical model establishes a relationship between the prestack seismic data and the unknown model parameters such as wavelet, velocity, density, and locations of interfaces. In this paper, we

use a 50 Hz zero-phase Ricker wavelet and keep it the same across the offset or angle for both PP and PS data.

By combining PP and PS reflection coefficients using least squares estimation, we can solve a system of equations for Vp, Vs, and ρ. The least-squares (LS) system is defined as

$$LS = \sum_{j=1}^m \sum_{i=1}^n [T_{PP}^*(\theta_i, t_j) - T_{PP}(\theta_i, t_j)]^2 + \sum_{j=1}^m \sum_{i=1}^n [T_{PS}^*(\theta_i, t_j) - T_{PS}(\theta_i, t_j)]^2 + \sum_{k=1}^l (m_k^* - m_k)^2 \quad (4)$$

Here, T_{PP} and T_{PS} are the synthetic model responses of the perturbed initial model. The values of T_{PP}^* and T_{PS}^* are the recorded seismic data. The summation is done over all incidence angles ($i=1,2,\dots,n$) and two-way times ($j=1,2,\dots,m$) for the PP and PS seismic data. $m_k = (V_{P1}, V_{S1}, \rho_1, V_{PN}, V_{SN}, \rho_N)$ are the petroelastic parameters of the first and last layer. $m_k^* = (2.6, 1.3, 2.4; 2.2, 1.1, 2.0)$ is, for example, the prior information for m_k . Note that in this paper, the velocity is in thousand m/s and density in gm/cc. Equation 4 is used for PP-PS joint inversion. We then remove the first term of equation 4 for PS only inversion or the second term for PP only inversion respectively. This least-squares problem is straightforward to solve by using SA or nonlinear CG. The details of SA and nonlinear CG methods can be found in many publications (Jean and Jorge, 1992; Goffe et al, 1994).

Tests, Results, and Observations

We construct a six-layer earth model as shown in Figure 1 and compute the synthetic model response as the input data using linearized Zoeppritz approximations in equations 1 and 2. We test the accuracy of the two inversion methods, the impact of input data type and combination, i.e., PP data only, PS data only or PP-PS data jointly, the influence of signal-to-noise-ratio and the sensitivity of initial model. Also we compare the computation efficiency between two optimizations SA and CG. The following selected figures highlight some of our tests.

First we evaluate the impact of inversion methods and input data type. Figure 1 displays the comparison of inverted Vp, Vs and ρ values of SA and CG methods using different input data types: a) PP data only, b) PS data only, and c) PP-PS data jointly. In the display, solid line is the actual model, dash-line is the SA result, and dot-line is the CG result. Also for all the figures hereon, the density value is reduced by 2 to fit in the display. The comparison shows that (1) one can reasonably invert all three parameters, Vp, Vs and ρ, from PP data only but not from PS data only, (2) CG result is slightly better than SA result if the initial model is not too far from the actual model, and (3) PP-PS joint inversion improves the result greatly.

Then we test the influence of signal-to-noise ratio using SA inversion. Figure 2 displays the comparison of SA inversion results using different random noise levels and input data types: a) PP data only, b) PS data only, c) PP-PS data jointly. In the display, solid line is the actual model, dash-line is the result with no noise, dot-line is the result with SNR = 4 dB, and dash-dot-line is the result with SNR = 1dB. The comparison shows that (1) the inversion result is not very sensitive to signal-to-noise ratio, (2) the inversion result of PP data only is less affected by the noises compared to that of PS data only, and (3) PP-PS joint inversion improves noticeably the result compared to that of PP only or PS only.

We follow up to test the sensitivity of the initial model using SA inversion, i.e., the input values and the contrast of Vp, Vs, and ρ between layers. Figure 3 is the comparison of SA inversion results using different initial modes and data types: a) PP data only, b) PS data only,

c) PP-PS data jointly. In the display, solid line is the actual model, dash-line is the result using an initial model with the maximum values of actual model, $V_p=2.6$, $V_s=1.3$, $\rho=2.4$, for all layers, dot line is the result using an initial model with the average values of actual model, $V_p=2.4$, $V_s=1.2$, $\rho=2.2$, for all layers, and dash-dot line is the result using an initial model with the minimum values of actual model, $V_p=2.2$, $V_s=1.1$, $\rho=2.0$, for all layers. The comparison shows that (1) the inversion result of PP-PS data jointly is the least sensitive to initial model, followed by PP only inversion, and then PS only inversion, (2) the non-uniqueness of V_p in the inversion of PS data only makes the result more sensitive to the initial model, and (3) PP-PS joint inversion is the most accurate solution, reduce the non-uniqueness nature of modeling, and is almost independent of the initial model.

Finally we test the sensitivity of the initial model using CG inversion. Figure 4 is the comparison of CG inversion results using different initial models and data types: a) PP data only, b) PS data only, and c) PP-PS data jointly. Line type legend and initial model values are the same as those in Figure 3. The conclusions are very similar to that of SA inversion in Figure 3 except that CG inversion is more dependent on the initial model than SA inversion even for PP-PS data jointly. However, CG inversion is much faster than SA inversion. For example, CG method is about 90 times faster than SA method for all input data types.

Conclusions

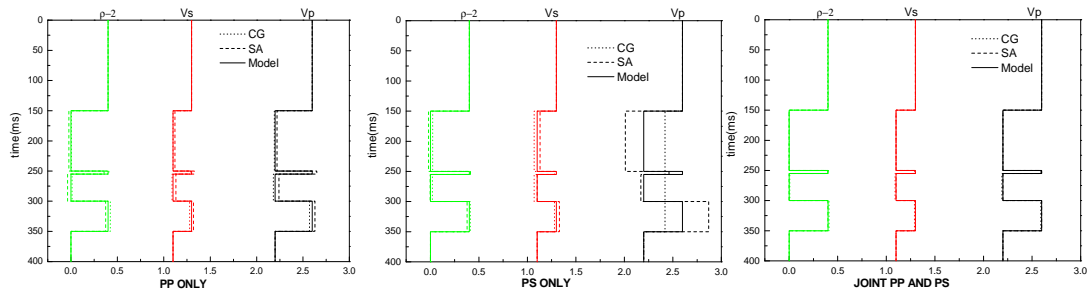
Two joint inversion methods based on SA and nonlinear CG methods using PP data only, PS data only and PP-PS data jointly are presented and evaluated with different controlled conditions. The absolute values of three petroelastic parameters, i.e., P-wave velocity V_p , S-wave velocity V_s , and bulk density ρ are inverted for a simple synthetic 1D model with different input data types, different signal-to-noise ratios, and different initial models without the constraint of V_s/V_p . The results show that (a) joint inversion is the more robust and accurate than PP or PS only inversion, (b) SA method is less dependent on the initial model than CG method, (c) both SA and CG methods are not sensitive to random noise, (d) CG computation is much faster than SA and can be used if the initial model is close to the actual geology. The result of this inversion test is promising. Further work on the methodology and the application of real data will be the logical next step.

Acknowledgements

The authors wish to thank Geotrace Technologies Inc. for permission to give this paper.

References

- Aki, K. and Richards, P. [1980] Quantitative Seismology, W.H. Freeman & Co.
- Goffe, W. L., Ferrier, G.D. and Rogers, J. [1994] Global optimization of statistical functions with simulated annealing. *Journal of Econometrics*, **60**, 65-100.
- Jean, C. G. and Jorge N. [1992] Global convergence properties of conjugate gradient methods for optimization. *Journal of Optimization*, **2**, 21-42.
- Rabben, T. E., Tjelmeland H. and Ursin B. [2008] Non-linear Bayesian joint inversion of seismic reflection coefficients. *Geophysical Journal International*, **173**, 265-280.
- Veire, H.H. and Landrø, M. [2006] Simultaneous inversion of PP and PS seismic data. *Geophysics*, **71**, R1-R10.

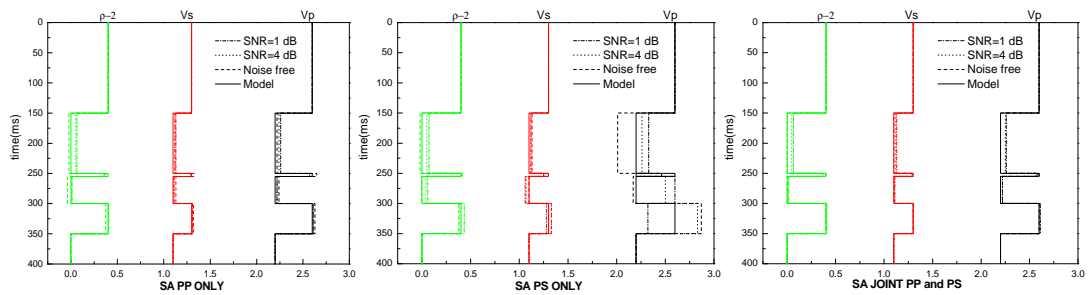


1a

1b

1c

Figure 1 Comparison of SA and CG inversion results using a) PP data only, b) PS data only, and c) PP-PS data jointly.

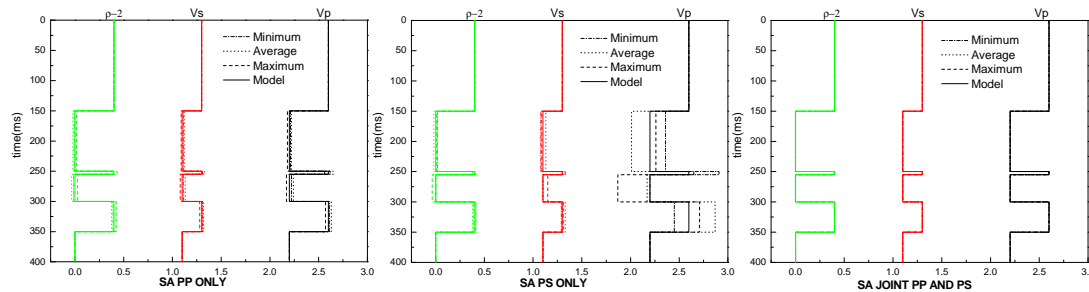


2a

2b

2c

Figure 2 Comparison of SA inversion results with different noise levels using a) PP data only, b) PS data only, and c) PP-PS data jointly.

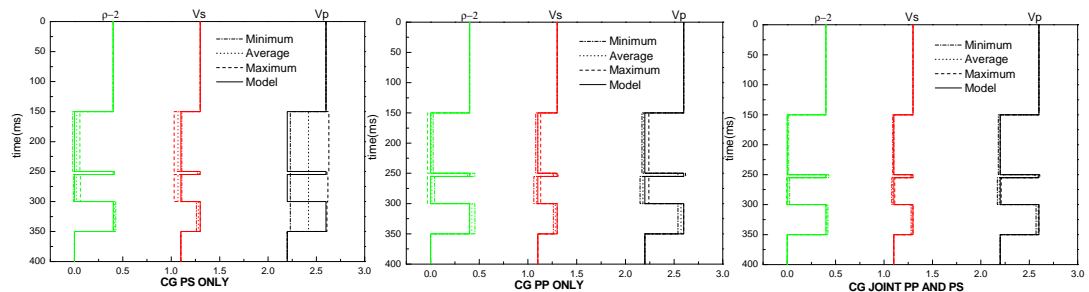


3a

3b

3c

Figure 3 Comparison of SA inversion results with different initial models using a) PP data only, b) PS data only, and c) PP-PS data jointly.



4a

4b

4c

Figure 4 Comparison of CG inversion results with different initial models using a) PP data only, b) PS data only, and c) PP-PS data jointly.